

# KINETICS OF GAS-PHASE REACTIONS RELEVANT TO THE CHEMICAL VAPOR DEPOSITION OF INDIUM COMPOUNDS

M. D. ALLENDORF, A. H. McDANIEL

Sandia National Laboratories, Livermore, CA 94551-0969, mdallen@sandia.gov

SAND--98-8468C  
CONF-9705242--

## ABSTRACT

The kinetics of trimethylindium pyrolysis are investigated in a flow reactor equipped with a molecular-beam mass-spectrometric sampling system. Data are analyzed using a new computational approach that accounts for heat and mass transport in the reactor. The measured activation energy, 46.2 kcal mol<sup>-1</sup>, is in good agreement with previously reported values.

## INTRODUCTION

**DISTRIBUTION OF THIS DOCUMENT IS UNLIMITED**

Compounds containing indium are of interest for electronic and optical applications. These compounds include III-V semiconductors such as InP and InAs used in both electronic devices and solar cells, and indium tin oxide, which can be used for optical memory and antireflection coatings. Chemical vapor deposition (CVD) techniques can be used to deposit these materials on a variety of substrates. At the temperatures typically employed (550 - 900 K), gas-phase chemical reactions involving the indium-containing precursor can occur. These reactions can be of two types: 1) pyrolysis of the original precursor, and 2) bimolecular reactions between the precursor or its decomposition products and other source gases, such as water, oxygen, ammonia, or phosphine. The rates of these reactions determine the identity of the molecules interacting with the substrate and, consequently, the deposition rate. They may also determine the extent to which impurities such as carbon are incorporated into the film. It is thus desirable to gain a more fundamental understanding of these reactions to provide data for detailed models used to simulate the growth process.

One commonly used indium-containing precursor is trimethylindium (TMI). The chemistry of this compound is a useful starting point for probing the reactivity of organometallic indium compounds for several reasons. First, its relatively high vapor pressure makes it easy to deliver to experimental apparatus. Second, although other precursors have been developed, their more complex structure adds to the difficulty of interpreting kinetic data. Third, the widespread use of TMI in the CVD of electronic materials makes the results of an investigation of its reactions of interest to a broad community. Finally, several investigators have studied TMI pyrolysis and their results are quite valuable in guiding the design of new experiments.

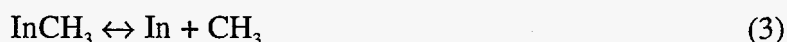
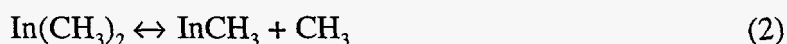
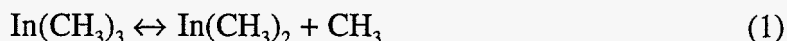
The submitted manuscript has been authored by a contractor of the United States Government under contract. Accordingly the United States Government retains a non-exclusive, royalty-free license to publish or reproduce the published form of this contribution, or allow others to do so, for United States Government purposes.

**MASTER**

## **DISCLAIMER**

**Portions of this document may be illegible electronic image products. Images are produced from the best available original document.**

The kinetics of TMI pyrolysis are far from being completely understood. The earliest experiments were reported by Jacko and Price (JP) [1], who observed the decomposition of TMI in a toluene carrier gas at pressures from 6 to 33.5 Torr and temperatures from 550 to 781 K. Their results suggest a mechanism in which methyl groups are sequentially lost from TMI in homogeneous gas-phase reactions:



At temperatures above 673 K, Reaction 2 is thought to be fast, resulting in rapid conversion of TMI to  $\text{InCH}_3$ . The measured rate constants for Reactions 1 and 3 each contain a small contribution from surface reactions. The JP results were later used to determine heats of formation and bond energies for the  $\text{In}(\text{CH}_3)_n$  species [2]. Buchan and Jasinski used these values to perform RRKM calculations predicting the fall-off behavior of Reaction 1 [3].

Larsen and Stringfellow (LS) measured the TMI pyrolysis rate by measuring weight gains in a tube [4]. An activation barrier of  $40.5 \text{ kcal mol}^{-1}$  was obtained in nitrogen carrier gas, which is lower than the  $47 \text{ kcal mol}^{-1}$  found by JP in toluene gas. A later investigation by Buchan, Larsen, and Stringfellow (BLS) produced an activation barrier in helium carrier gas of  $54.0 \text{ kcal mol}^{-1}$  [5]. Like JP, these investigators determined that heterogeneous processes had a small effect on their measured rates, but did not correct for this. More recently, Sugiyama et al. measured TMI decomposition in hydrogen [6]. Their rate constant is a factor of two slower than BLS rate in hydrogen; however, they detected only methane in the products, while BLS detected both ethane and methane.

These results indicate that the details of TMI pyrolysis are still unclear. In particular, the variation in the measured activation energies, which range from  $40.5$  to  $54.0 \text{ kcal mol}^{-1}$ , is problematic, especially since these data are the only information available that can be used to estimate heats of formation for methyl-indium compounds. In addition, the effects of radical scavengers in an inert carrier gas have not been explored (JP conducted their experiment in toluene vapor without additional carrier gas).

In this paper, we describe a high-temperature flow reactor equipped with a molecular-beam mass-sampling apparatus that can be used to characterize the reactions of CVD precursors. We also discuss a new numerical method for analyzing flow-reactor data that accounts for non-uniform radial and axial concentration and temperature profiles in the reactor. These methods are used to conduct an initial investigation of the pyrolysis of TMI in helium. Because of the high sensitivity of our detection system, we are able to use lower TMI concentrations (300 ppm) than were accessible to previous investigators, thus minimizing the impact of secondary reactions.

Finally, the TMI decomposition rate was measured with and without an excess of toluene to determine the importance of radical-chain mechanisms.

## EXPERIMENT

The experimental apparatus is shown schematically in Figure 1 and consists of a high-temperature flow reactor (HTFR) interfaced to a molecular-beam mass spectrometer. The HTFR is a water-jacketed steel chamber that contains alumina- and graphite-felt insulation (not shown), heating elements, a flow tube, a ceramic heat-exchanger, and a translating injector. The flow tube is constructed of quartz and has an internal diameter of 6.4 cm and an overall length of 112 cm. Three independently controlled graphite heating elements control the temperature of the tube. A movable injector, constructed of stainless steel and surrounded by a water jacket to prevent decomposition of thermally sensitive reactants, allows the residence time of the injected gas(es) to be changed. Residence times up to 2000 ms can be achieved by adjusting the injector position, gas flow rate, pressure, and temperature. Mass-flow controllers are used to meter all gas feed rates. The reactor exhaust is throttled, allowing for feedback control of the reactor pressure to any desired setpoint within the range 1 to 700 Torr.

Gases exiting the flow tube are sampled using a modulated molecular-beam mass spectrometer, shown in Figure 1. Expansion through the 125- $\mu$ m sampling nozzle is supersonic and under-expanded so that, within 2-5 nozzle diameters, the flow becomes rotationally cold and collisionless, "freezing" the chemical composition of the mixture. This allows transient or short-lived species to be detected as well as stable compounds. The molecular beam thus formed is chopped with a resonant modulator driven at 200 Hz. The chopper reference and analog multiplier signals are routed through a lock-in amplifier where the modulated ion signals are extracted from the DC baseline. This allows for discrimination between beam gases and quiescent gases that are present in the mass-spectrometer chamber. Phase-sensitive detection reduces the ultimate detection limit to less than 1 ppm at reactor pressures above 5 Torr in a helium carrier gas. The mass-spectrometer (Extrel C50) has a unit resolution up to 500 AMU.

The pyrolysis of TMI was investigated at temperatures between 523 and 698 K in He carrier gas at a reactor pressures of 10.0, 15.0, and 20.0 ( $\pm$  0.2) Torr. TMI (Epichem; electronic grade) was fed by passing helium (100 - 300 sccm) through a manufacturer-supplied container that was maintained at a temperature of 298 K to yield a vapor pressure of 2.5 Torr. It was used without further purification. Conditions for the various experiments performed are given in Table I. Toluene vapor was delivered by using the vapor pressure of the liquid at 333 K to drive a mass-flow controller. A typical experiment involved recording the intensity of the desired ion signals at 5 to 10 injector positions, ranging from 225 to 425 mm from the sampling nozzle. The decay of TMI and formation of products was observed by monitoring the

signal at the following mass/charge ratios ( $m/e$ ): 145 ( $\text{In}(\text{CH}_3)_2^+$ ), 115 ( $\text{In}^+$ ), 26-30 ( $\text{C}_2^+$  hydrocarbons), 16 ( $\text{CH}_4^+$ ), and 15 ( $\text{CH}_3^+$ ). The parent ion of TMI was never observed.

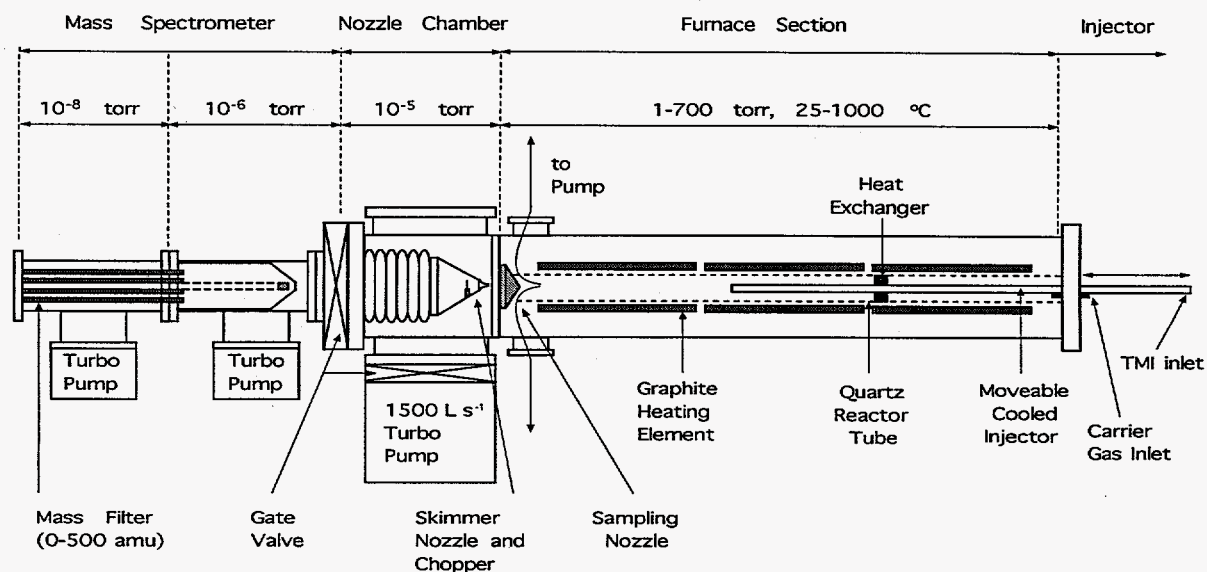


**Figure 1.** Schematic of the high-temperature flow reactor (HTFR).

Table I. Experimental conditions

$P_{\text{tot}}$ (torr)	$Q_{\text{tot}}$ (sccm) <sup>a</sup>	Temp. (K)	$\Delta\tau$ (s) <sup>b</sup>	[TMI] (ppm)	[Toluene] (ppm)	IE (eV) <sup>c</sup>
20.0	1200	523 - 698	0 - 0.60	300	0	70
15.0	2000	523 - 698	0 - 0.15	300	$2 \times 10^4$	70
10.0	2000	648	0 - 0.15	750	0 or $2 \times 10^4$	24

<sup>a</sup> Total flow rate. <sup>b</sup> Average relative gas residence time, based on furnace set-point temperature.

<sup>c</sup> Ionization energy.

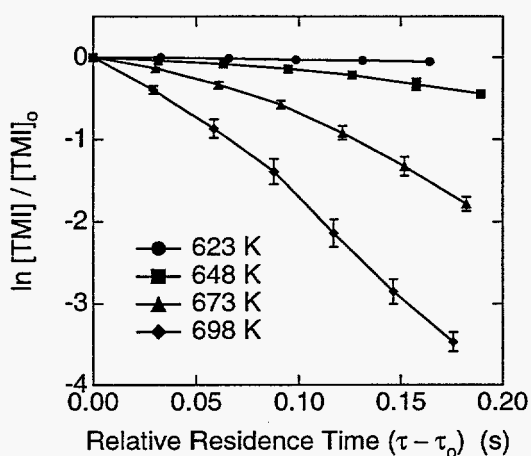
## RESULTS

Figure 2 shows the time-dependence of the  $m/e$  145 signal corresponding to the  $\text{In}(\text{CH}_3)_2^+$  ion as a function of reactor temperature. The reaction is a strong function of temperature, as observed by all previous investigators [1,4-6]. The only products that can be conclusively identified are methane ( $\text{CH}_4$ ) and ethane ( $\text{C}_2\text{H}_6$ ).

Plots of the type shown in Figure 2 should be linear in the ideal case of a single first-order or pseudo-first-order reaction in an isothermal reactor. Under these conditions, the rate constant for the reaction is equivalent to the slope of the line. As can be clearly seen from these data, however, there is a substantial amount of curvature in these plots, making a straightforward analysis of the data impossible. Figure 3, in fact, shows an attempt to fit a line to the data at 648 K; the agreement is quite poor. Several factors could contribute to this behavior: 1) the signal being plotted may have contributions from more than one species; 2) more than one

reaction may be occurring in the reactor; and 3) the temperature profile of the reactor may be non-uniform. Since it is possible that all three factors are involved, we address each one in detail below.

As discussed in the introduction, evidence of previous investigations suggests that TMI undergoes sequential loss of methyl radicals. The mass of the initial product,  $\text{In}(\text{CH}_3)_2$ , is the same as the mass of the primary ion fragment of TMI formed in the mass spectrometer. As a consequence,  $m/e$  145 could have contributions from both the reactant and product. Since the mass spectrum of  $\text{In}(\text{CH}_3)_2$  is unknown, it is not possible to determine the individual contributions to the  $m/e$  145 from  $\text{In}(\text{CH}_3)_2$  and TMI. Unfortunately, all other TMI fragments are affected in the same manner. Evidence presented by JP suggests, however, that the  $\text{In}(\text{CH}_3)_2$  molecule rapidly decomposes unimolecularly to form  $\text{InCH}_3$ . Thus, its steady-state concentration is likely to be very small. For this reason, we assume here that the only contribution to  $m/e$  145 comes from TMI.



**Figure 2.** Temperature dependence of TMI concentration as a function of residence time

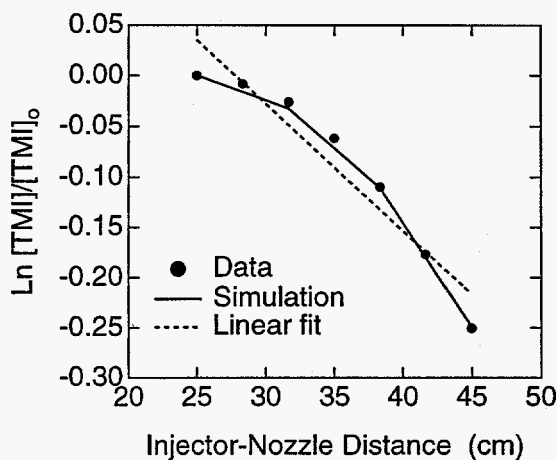
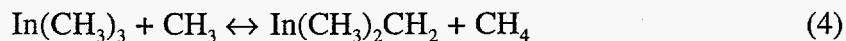


**Figure 3.** 648 K data from Fig. 2 fit by linear least-squares method and by CRESLAF model.

Since the products of Reaction 1 are both radicals, the possibility exists for radical-chain mechanisms to accelerate the decomposition of TMI. In particular,  $\text{CH}_3$  could extract a hydrogen atom from TMI to form  $\text{CH}_4$ :



That this could occur is suggested by our observation of methane in the product gases in the absence of toluene. The resulting indium radical,  $\text{In}(\text{CH}_3)_2\text{CH}_2$ , could then react with other TMI molecules or radicals to form low-volatility polymers that would be lost to the reactor walls.

Although the rate of this abstraction is unknown, it is reasonable to assume, based on the bond energies of other Group III alkyls [5], that the C-H bond strength is essentially unaffected by the bonding of the carbon with indium. Thus, the rate of hydrogen abstraction from TMI should be similar to that for hydrocarbons, such as ethane. Under this assumption, we estimate a rate constant for Reaction 4 of  $\sim 2 \times 10^8 \text{ cm}^3 \text{ mol}^{-1} \text{ s}^{-1}$  at 648 K (which is in the middle of our experimental temperature range). Whether or not this reaction affects the rate of TMI decomposition depends on the rate of recombination of methyl radicals to form ethane ( $\text{C}_2\text{H}_6$ ), which is also an observed product. Since the rate constant for this reaction is well known [7], we can compare its rate with that of Reaction 4. At 648 K and 10 torr, the rate of methyl radical recombination is nearly  $7 \times 10^4$  times faster than Reaction 4. Thus, Reaction 4 should have little impact on the observed rate. As will be seen below, this is further supported by the lack an effect of toluene, a radical scavenger, on the rate constant.

The third and remaining possibility is that the non-linearity in Fig. 2 is caused by temperature non-uniformities in the HTFR. Fig. 4 shows the centerline temperature profile, measured with a type-K thermocouple, for two different positions of the water-cooled injector. The temperature profile is far from flat as a result of heat losses induced by the water-cooled injector and in the unheated portion of the flow tube at its downstream end. At locations near the injector (for example, 190-230 mm for an injector-sampling nozzle distance of 225 mm), the temperature is as much as 38 K below the setpoint. Between 0 and 100 mm, the temperature drops as the gases flow through an unheated section of the reactor. These variations change the rate of TMI pyrolysis as a function of residence time, thereby inducing curvature in the  $\ln(\text{concentration})$  vs. residence time plots.

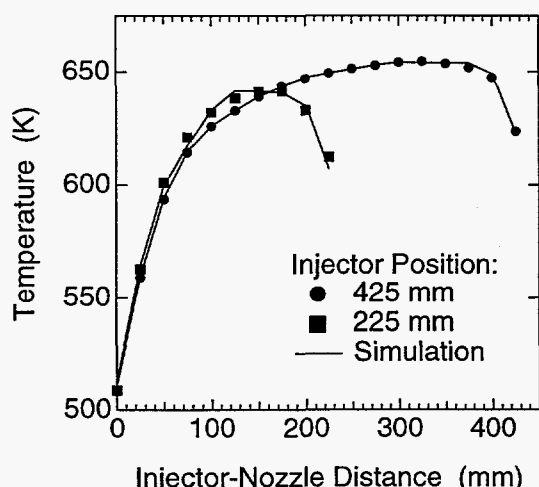


**Figure 4.** Measured and predicted (by the CRESLAF model) axial temperature profiles in the HTFR.

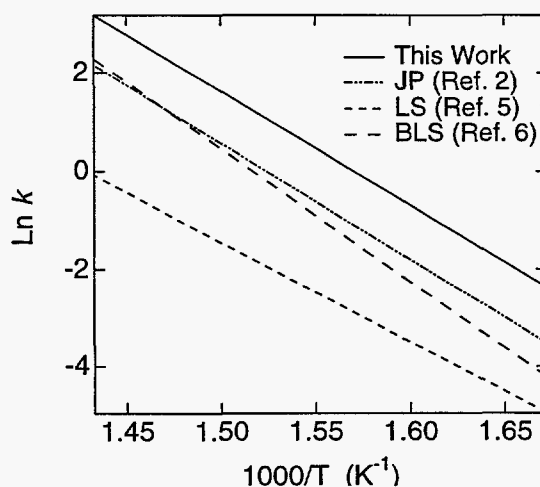


**Figure 5.** Comparison of literature rate expressions for TMI pyrolysis with results of this work.

To extract an accurate rate constant for TMI pyrolysis, we developed a new approach to the analysis of flow-reactor data by combining the non-linear least-squares fitting program TJMAR [8] with the CRESLAF two-dimensional boundary-layer model of the reactor. CRESLAF includes both gas-phase and surface chemical reactions [9], as well as radial diffusion, axial convection, and heat transfer. We must assume that the injected gases, which represent only 10-15% of the total flow, mix and reach the temperature of the preheated carrier gas instantaneously. This is necessary because the CRESLAF code simulates only the flow of premixed gases through a tube. Under the low-pressures used here and using a helium carrier gas, diffusion rates are sufficiently high to make this a reasonable assumption. The axial temperature profile predicted by the model for two different injector positions is compared in Figure 4 with the measured profile; good agreement is achieved.

To determine the rate for Reaction 1, a 21-step gas-phase reaction mechanism was used that includes Reactions 1 and 2 as well as eighteen other reactions involving only hydrocarbon species. (Due to space constraints, the full mechanism is not presented here.) The latter include methyl-radical recombination, hydrogen abstraction from toluene by methyl, and formation of methane, ethane, ethylene, and ethylbenzene products. Rate constants and thermochemistry for the hydrocarbon reactions are well known and were taken from standard sources [7]. Reaction 2 was assumed to be very fast relative to Reaction 1 ( $k_2 = 1.0 \times 10^{16} \text{ s}^{-1}$  at all temperatures). Reaction 3 was not included, since results of JP indicate that it is very slow under the conditions of our experiments. Thus, only the rate constant of Reaction 1 was fitted by the model.

The fit to the measured TMI concentration (based on the signal at  $m/e$  145) is shown in Figure 3 and is quite good. The rate constant obtained by fitting data measured at a single furnace setpoint of 648 K is  $k_1 (\text{s}^{-1}) = 7.00 \times 10^{15} \exp(-46,170/RT)$ . This can be compared with  $k (\text{s}^{-1}) = 2.8 \times 10^{16} \exp(-47,700/RT)$  obtained from a simple linear least-squares fit (dotted line, Fig. 3). At 648 K, the linear fit yields a rate that is 22% higher than the one predicted by the detailed model. Realistically, this difference may be within the systematic experimental uncertainty. However, the magnitude of the effects caused by temperature gradients in the reactor increases as the furnace setpoint increases. This can be seen in Fig. 2; the curves obtained at higher temperatures curve more than those obtained at lower temperatures. Thus, the CRESLAF analysis will provide more accurate results when data are obtained over a broad range of temperatures.

Comparison of this work with the literature indicates that the activation energy obtained,  $46.2 \text{ kcal mol}^{-1}$ , is in the middle of the range of reported values ( $40\text{-}54 \text{ kcal mol}^{-1}$ ) and agrees well with the earlier measurement of JP. However, the decomposition rate is higher than those reported previously. The available rate expressions are plotted in Figure 5 along with the one derived here. At 648 K, the rate we obtain is almost a factor of three faster than JP and a factor of four faster than BLS. The reason for this is unclear. A heterogeneous component to the



reaction is one possible cause. However, experiments in which S/V was varied [1,5,6] or the chemical properties of the surface were changed [6] exhibited little or no effect on the rate. This would seem to rule out surface reactions. Our reactor also has the lowest surface/volume (S/V) ratio of those reported (S/V this work = 0.63; JP is unknown; BLS = 10; Sugiyama et al. = 2.5), so surface processes should be even less of a factor.

Experiments in which 20,000 ppm of toluene, a radical scavenger, were added to the reactant gases indicate that reactions involving product species such as  $\text{CH}_3$  (e.g., Reaction 4) do not contribute significantly to the observed rate of TMI decomposition. No effect, within experimental error, was observed upon addition of toluene. This result is consistent with the use of low TMI concentrations in our experiments (300 ppm) to minimize the impact of secondary reactions on the observed rate. Given these low concentrations and the fact that, like all previous studies of TMI decomposition, we used a flow reactor, there is no reason to believe that radical reactions should be any more important in our experiments than the previous investigations. Thus, such processes cannot be invoked to explain the faster rates of TMI decomposition that we observe.

To summarize, we have developed new experimental and analytical techniques that should lead to improved understanding of the chemistry of organometallic compounds such as TMI. A valuable feature of the new approach to flow-reactor data analysis is that it enables one to measure a reaction's temperature dependence by conducting a single experiment, rather than a series of experiments at different temperatures. This is possible because the gases are exposed to a range of temperatures as they travel through the HTFR and the analysis does not assume that the temperature profile is uniform. Thus, when one would like to obtain a broad picture of a molecule's reactivity, activation energies for a series of related reactions could be obtained (e.g., TMI +  $\text{NH}_3$ ,  $\text{PH}_3$ , or  $\text{AsH}_3$ ) with a relatively small number of experiments.

Although the limited extent of our TMI pyrolysis data is sufficient to demonstrate only the capabilities of our methods, investigations underway will provide the data required to resolve outstanding questions associated with TMI pyrolysis. We are also developing *ab initio* methods to predict heats of formation for indium-containing compounds, which will provide insight into the energetics of possible gas-phase reactions.

#### ACKNOWLEDGMENTS

The authors are grateful for the support of this research provided by Libbey-Owens-Ford Co. (Toledo, OH) and the U.S. Dept. of Energy, Office of Industrial Technologies.

## REFERENCES

1. M. G. Jacko, S. J. W. Price *Can. J. Chem.* **42**, 1198 (1964).
2. W. D. Clark, S. J. W. Price *Can. J. Chem.* **46**, 1634 (1968).
3. N. I. Buchan, J. M. Jasinski *J. Cryst. Growth* **106**, 227 (1990).
4. C. A. Larsen, G. B. Stringfellow *J. Cryst. Growth* **75**, 247 (1986).
5. N. I. Buchan, C. A. Larsen, G. B. Stringfellow *J. Cryst. Growth* **92**, 591 (1988).
6. M. Sugiyama, et al. *Appl. Surf. Sci.* **117/118**, 746 (1997).
7. *NIST Chemical Kinetics Database, Version 6.0.*
8. T. H. Jefferson, "TJMAR1-A Fortran Subroutine for Nonlinear Least Squares Parameter Estimation," Sandia National Laboratories Report, SLL-73-0305, 1973.
9. M. E. Coltrin, et al., "CRESLAF (Version 4.0): A Fortran Program for Modeling Laminar, Chemically Reacting, Boundary-Layer Flow in Cylindrical or Planar Channels," Sandia National Laboratories Report, SAND93-0478 UC-401, 1996.